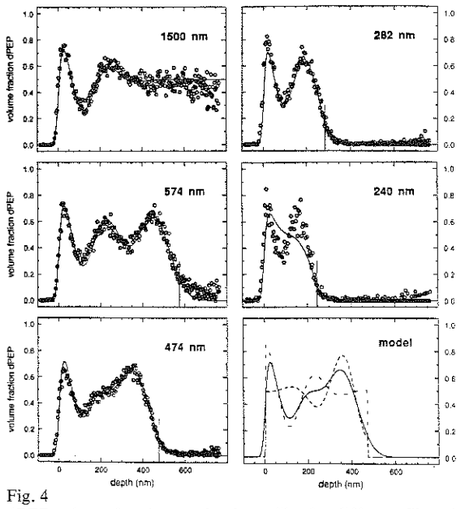

Fig. 4
dPEP volume fraction vs. depth profiles for different films thicknesses d as determined by NRA: (a) $d > 1000$ nm, (b) $d = 574$ nm, (c) $d = 474$ nm, (d) $d = 282$ mm, (e) $d = 240$ nm. The solid lines represent the model (f) discussed in the text, convoluted with a Gaussian of increasing full width at half maximum. The locations of the Si substrates are indicated by the vertical lines. (All substrates were stripped from oxide prior to film deposition)

the film thickness matches about 1.5 times the characteristic wavelength of the surface spinodal waves (Fig. 4d). We can easily model these results by superposing two damped cosines originating at the two boundary surfaces of the films with all parameters but the film thickness kept constant (solid lines in Fig. 4). This is shown in Fig. 4f for the particular film thickness realized in Fig. 4c. The model no longer describes the experimental data, however, when the film thickness is further decreased. This discrepancy can be seen in Fig. 4e and is observed in all samples thinner than about 280 nm. To understand this effect, we may compare the total film thickness to the most probable wave length at early times. As the wave vectors of the surface spinodal waves approach the bulk value at $t = 0$, we may extrapolate the data for $q_{\mathrm{m,bulk}}$ obtained from light scattering experiments on bulk PEP/dPEP samples [14] to $t = 0$. We estimate $q_{\mathrm{m,bulk}}(t=0) = 3.6 \times 10^{-3}$ Å^{-1} for $T = 321$ K, corresponding to $\lambda_{\mathrm{m}}(t=0) = 174$ nm. Since the substrate surface is covered by a PEP-rich layer in contrast to the polymer/vacuum interface, a minimal film thickness of $d_{\min} = 1.5 \cdot \lambda_{\mathrm{m}}(t=0) = 261$ nm is needed in order to realize a composition wave with $q_{\mathrm{m,bulk}}(t=0)$. As the film thickness falls below this limit, the system is forced to decompose with a larger characteristic wave vector, which then is determined by the macroscopic dimensions of the film.

Finally, we shall mention that the above results on the thickness dependence are in quantitative agreement with cell-dynamical simulations, mapped on the polymer system under consideration [6, 10]. With a detailed discussion being beyond the scope of this paper, it is worth mentioning that the results of such (three-dimensional) simulations can be used to investigate the in-plane morphology of samples showing the interference effects described above. It was shown that 'destructive interference' of the spinodal waves corresponds to the existence of a region close to the center of the film consisting of a large number of droplets of either of the two phases. This occurs in Fig. 4c and can be understood as the compromising reaction of the system to competing surface fields which tend to enrich the particular layer by one and the other phase at the same time. The resulting disorder disappears as soon as the film thickness approaches a value where both surface fields favor the same phase to be enriched at any given plane in the film (Fig. 4d). 'Constructive interference' therefore corresponds to an almost perfectly layered structure.

In summary, we have investigated the effects of the boundary surfaces on the spinodal decomposition in thin films of a binary polymer mixture. The surface layer formed during the decomposition process was found to follow a $t^{1/3}$ growth law in accordance with recent theoretical predictions. For sufficiently thin films, it was shown that the entire phase morphology can be determined by surface effects.

This work was supported by the NSF-DMR Polymer Program Grant No. DMR-8719123. One of us (G.K.) greatly appreciates financial support through the Max-Kade-Foundation, New York. F.S.B. is indebted to the NSF for support through Grant No. DMR-8957386. We thank L.J. Norton, M.H. Rafailovich, and J. Sokolov for helpful discussions. The authors are grateful to J.F. Marko and A. Chakrabarti for sharing some of their unpublished results. The skillful help of N. Szabo and P. Revesz during the course of the experiments is gratefully acknowledged.

References

[1] R.C. Ball and R.L.H. Essery, J. Phys. Condens. Matter *2*, 10303 (1990).
[2] R.A.L. Jones, L.J. Norton, E.J. Kramer, F.S. Bates, and B. Wiltzius, Phys. Rev. Lett. *66*, 1326 (1991).
[3] F. Bruder and R. Brenn, Phys. Rev. Lett. *69*, 624 (1992).
[4] A. Cumming, P. Wiltzius, F.S. Bates, and J.H. Rosedale, Phys. Rev. A *45*, 885 (1992).
[5] H. Tanaka, Phys. Rev. Lett. *70*, 53 (1993); Phys. Rev. Lett. *70*, 2770 (1993).
[6] G. Krausch, C.-A. Dai, E.J. Kramer, J.F. Marko, and F.S. Bates, Macromolecules *26*, 5566 (1993).
[7] G. Krausch, C.-A. Dai, E.J. Kramer, and F.S. Bates, Phys. Rev. Lett. *71*, 3669 (1993).
[8] G. Brown and A. Chakrabarti, Phys. Rev. A *46*, 4829 (1992).
[9] S. Puri and K. Binder, Phys. Rev. A *46*, R4487 (1992).
[10] J.F. Marko, Phys. Rev. E *48*, 2861 (1993).
[11] F.S. Bates, J.H. Rosedale, H.E. Bair, and T.P. Russell, Macromolecules *21*, 1086 (1988).
[12] J. Sokolov, M.H. Rafailovich, R.A.L. Jones, and E.J. Kramer, Appl. Phys. Lett. *54*, 590 (1989).
[13] U.K. Chaturvedi, U. Steiner, O. Zak, G. Krausch, G. Schatz, and J. Klein, Appl. Phys. Lett. *56*, 1228 (1990).
[14] U. Steiner, J. Klein, E. Eiser, A. Budkovski, and L.J. Fetters, Science *258*, 1126 (1992).

Presented at the Discussion Meeting of the Deutsche Bunsen-Gesellschaft für Physikalische Chemie "Phase Transitions at Interfaces" in Bad Herrenalb, September 22nd to 24th, 1993 E 8558

Dynamical Formation of Metastable Phases at Interfaces

Hartmut Löwen

Sektion Physik der Universität München, Theresienstr. 37, D-80333 München, Germany

Key Words: Crystal Growth / Interfaces / Nonequilibrium Phenomena / Phase Trnasitions / Surfaces

A Ginzburg-Landau model of non-conserved order parameter dynamics is analyzed. The model involves three different phases: a stable high-temperature phase, a stable low-temperature phase and a metastable phase. It is shown that a macroscopic portion of metastable phase can be formed by a dynamic instability which splits the front separating the stable high- and low-temperature phases. The presence of an external field blocks this metastable phase formation and leads to a non-monotonic behaviour of the metastable phase portion as a function of time.

Usually metastable phases are produced by fast temperature quenches. The common picture is that due to kinetic obstacles the stable phase does not have enough time to form and a macroscopic portion of metastable phase can be created. There are many concrete examples of metastable phases in physics and metallurgy [1] and for more than a century [2] experimental and technical experience on creating metastable crystalline structures and glasses from the melt has accumulated. It is, however, only recently that *theoretical* mechanisms have been studied. Two general mechanisms have been proposed [3]: First, the *nucleation* rate of metastable germs may be larger than that of stable germs. Second, the *growth* rate of the metastable phase exceeds that of the stable phase.

It is the purpose of this article to review briefly a *third* mechanism for the formation of a metastable phase which was proposed recently [4–6]. The corresponding scenario is that upon rapid cooling the metastable phase nucleates at the *growing interface* between the stable high-temperature phase (0) and the stable low-temperature phase (2) and then grows faster than the stable low-temperature phase. This is directly connected to a *splitting instability* of the 02-front which splits into two independent 01 and 12 interfaces both of which moving with a different velocity such that a macroscopic portion of the metastable phase can be formed dynamically.

To see the splitting instability in its simplest setting we follow Ref. [4] and consider usual Ginzburg-Landau dynamics for a one-component non-conserved dimensionless order parameter $q(x,t)$ (alias model A without noise). Interfacial dynamics is studied in one spatial dimension x as a function of time t. In the one-dimensional geometry any roughening effects are neglected. The relaxational equations for the order parameter dynamics read

$$\frac{\partial q(x,t)}{\partial t} = -\Gamma \frac{\delta \mathscr{F}[q(x,t)]}{\delta q} \tag{1}$$

with the free energy functional

$$\mathscr{F}[q(x,t)] = \int_0^\infty \mathrm{d}x \left[\frac{\varepsilon \lambda}{2} \left(\frac{\partial q(x,t)}{\partial x} \right)^2 + \frac{\varepsilon}{\lambda} f(q(x,t)) \right] . \tag{2}$$

Here, λ is a microscopic bulk correlation length which determines the length scale, ε sets the energy scale and Γ is an Onsager coefficient which sets the time scale. In the following, all quantities are measured in these natural units.

To get explicit results we make the following concrete choice for the free energy density $f(q)$:

$$\frac{\mathrm{d}f}{\mathrm{d}q} = q(q-(0.5-b))(q-1)(q-1.5)(q-2) \tag{3}$$

with a control parameter $b \propto (T_{02} - T)$ where T_{02} is the coexistence temperature between two stable phases (0) and (2). Later on we shall briefly discuss how the explicit form of $f(q)$ influences the splitting instability. As can be clearly seen in Fig. 1 where $-f(q)$ is shown for different control parameters b, *three* phases are involved:

a) the stable high-temperature phase (0) (e.g. liquid) chosen to be at $q = 0$;
b) the stable low-temperature phase (2) (e.g. crystal) chosen to be at $q = 2$;
c) a metastable phase (1) lying at $q = 1$ in between the two stable phases.

We are now looking for dynamical solutions $q(x,t)$ of (1) with an arbitrary initial profile and boundary conditions

$$\lim_{x \to -\infty} q(x,t) = 2 \tag{4}$$

$$\lim_{x \to \infty} q(x,t) = 0 \tag{5}$$

for all $t \geq 0$. In order to get an insight into the splitting instability let us discuss the existence of *steady state solutions* between the phases 01, 12 and 02. These are profiles moving with a *constant* interface velocity, v_{01}, v_{12} resp. v_{02}. In terms of steady state velocities the scenario of the splitting instability can be understood as follows [4]: If $v_{12} > v_{01}$ then steady state motion of the 02-interface is possible with a velocity v_{02} lying between v_{01} and v_{12}. On the other hand, for $v_{12} < v_{01}$ there is no steady state solution for the 02-interface. The 02-interface splits into two independent 01 and 12 interfaces which move asymptotically for large times

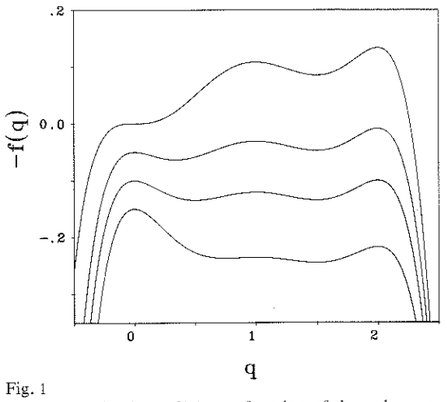

Fig. 1
Free energy density $-f(q)$ as a function of the order parameter q for different control parameters $b \propto (T_{02} - T)$. The curves are shifted by an arbitrary constant. From up to down the values of b are as follows:
a) $b = 0.5$, liquid spinodal line
b) $b = b_c = 0.15419$, critical value for interface splitting
c) $b = 0$, coexistence between phase 0 and 2
d) $b = -0.25$, region where phase 0 is stable.

with their corresponding steady state velocities v_{01}, v_{12}. Since $v_{01} > v_{12}$ the metastable phase front grows faster into the unstable phase (0) than the stable phase grows into the metastable phase and a *macroscopic* portion of metastable phase is created dynamically. This portion grows linear in time $\propto (v_{01} - v_{12})t$. For $v_{12} = v_{01}$ the splitting transition occurs. The actual value of the steady state velocities directly depends on the detailed shape of $f(q)$. This implies that there is a critical control parameter b_c corresponding to $v_{12} = v_{01}$. For the concrete choice (3), the value of b_c is 0.15419. For $b \nearrow b_c$ the width of the 02 steady state front diverges indicating a dynamical prewetting by the metastable phase.

In Fig. 2, the width $w(t)$ of the metastable phase intervening between the stable high- and low-temperature phases is shown as a function of time t for different control parameters b. For $b < b_c$, in the steady state regime, it converges to a finite microscopic value; for $b \nearrow b_c$ it diverges logarithmically $\propto \ln(b_c - b)$; and for $b \geq b_c$ it diverges to even macroscopic values. Also, in the inset of Fig. 2, the time evolution of a typical order parameter profile is shown clearly showing the buildup of the metastable phase.

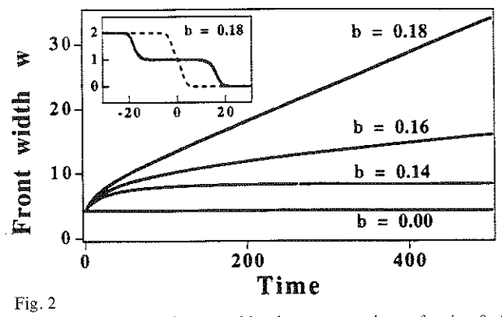

Fig. 2
Width of the layer of metastable phase versus time t for $b = 0$, 0.14, 0.16, and 0.18. Note that the critical control parameter is $b_c = 0.15419$. Inset: Splitting of the 02 front for $b = 0.18$. Order parameter q versus position x. The dashed curve is the initial stationary solution for $b = 0$. The solid curve shows a profile for $t = 10000$ time units

The same splitting effect is also possible for several order parameters. The case of two non-conserved order parameters was explicitly examined by Tuckerman and Bechhoefer [5].

The splitting instability is non-generic. Whether it occurs or not depends on the detailed form of the free energy density $f(q)$. In our chosen form (3), it does occur but in other choices it does not. We simply mention that the choice (3) represents a typical one with realistic free energy differences and typical undercoolings. Thus in certain systems one should see the splitting instability and in other ones one should not.

There are a number of possible mechanisms that limit the growth of the metastable phase in reality. One of them is an external field which is coupled to the order parameter. If the order parameter is simply a scaled particle number density, a gravitational field can be regarded as such a disturbing external field but other examples are also conceivable. The Ginzburg-Landau model is readily generalized to the case of a constant external field by adding the term $\alpha q x$ to the free energy density function $f(q)$ which thus becomes position dependent. α plays the role of a coupling parameter. Furthermore we now take a semi-infinite geometry $x \geq 0$. For different shapes of $f(q)$, Bocquet and the author have solved numerically the time evolution of the order parameter profile in an external field [6]. The results depend on the fact whether for $\alpha = 0$ the interface motion is in the steady state regime or in the regime where the splitting instability occurs.

In the first case the interface motion is first steady state like and then slows down due to the presence of the external field. For very large times, it approaches its equilibrium profile where the 02-interface position is positioned at a fixed x_0. x_0 decreases for increasing α. For large times, the interface position approaches x_0 exponentially in time, i.e. $\propto \exp(-t/\tau)$ with a characteristic decay time τ.

In the second case the width of the metastable phase first grows up to a maximal width w_{max}. w_{max} increases with decreasing coupling α and can even reach mesoscopic values. Then the width shrinks back again to a microscopic layer exponentially in time. This interesting *non-monotonic* behaviour of the width $w(t)$ is shown in Fig. 3 for three different parameter combinations, two of them being in the regime where the splitting instability occurs for $\alpha = 0$.

Some final remarks concern a possible experimental verification in real growth experiments. One possibility is to study dynamics of surface melting which was in a similar framework discussed by the author and Lipowsky [7]. Liquid crystalline systems often provide a number of metastable phases upon undercooling and may constitute ideal candidates for an experimental verification of the splitting instability [8]. Some unusual large layer thicknesses were observed at growing liquid-solid interfaces of atomic materials by Bilgram and coworkers [9] which may be related to the splitting instability. However, the latter experiments may also be explained by diffusing gas microbubbles, see e.g. [10]. Another promising system are colloidal suspensions where dynamics happens on a much larger timescale than for atomic systems. Here effects of an external field on a growing metastable phase may also be detectable (for a possible experiment with different metastable phases see [11]).

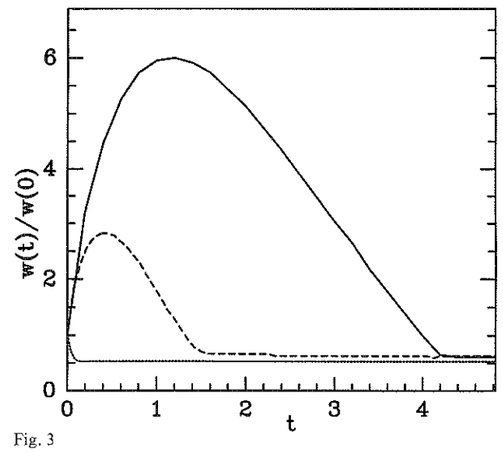

Fig. 3
Width of the layer of metastable phase, $w(t)$, versus time t for $\alpha = 0.8$ (solid line), $\alpha = 2$ (dashed line), and $\alpha = 1$ (dotted line). The form of $f(q)$ is chosen such that the solid and dashed lines are in the regime where the metastable phase forms by the splitting instability in the field-free case whereas the dotted curve is in the steady-state regime. The width is measured in terms of the width $w(0)$ of an arbitrarily chosen initial profile

References

[1] T.R. Anantharaman and C. Suryanarayana, J. Mat. Sci. *6*, 1111 (1971).
[2] W. Ostwald, Z. Phys. Chem. *22*, 289 (1987).
[3] W.J. Boettinger and J.H. Perpezko, "Fundamentals of rapid solidification," in: S.K. Das, B.H. Kear, and C.M. Adam (eds.) Rapidly Solidified Crystalline Alloys, p. 25, The Metallurgical Society of AIME, 1985.
[4] J. Bechhoefer, H. Löwen, and L.S. Tuckerman, Phys. Rev. Lett. *67*, 1266 (1991).
[5] L.S. Tuckerman and J. Bechhoefer, Phys. Rev. A *46*, 3178 (1992).
[6] L. Bocquet and H. Löwen, Phys. Rev. E (1993) in press.
[7] H. Löwen and R. Lipowsky, Phys. Rev. B *43*, 3507 (1991).
[8] J. Bechhoefer, A.J. Simon, A. Libchaber, and P. Oswald, Phys. Rev. A *40*, 2042 (1989); P. Oswald, J. Bechhoefer, A. Libchaber, and F. Lequeux, Phys. Rev. A *36*, 5832 (1987); P. Ribière, P. Ostwald, J. Phys. (Fr.) *51*, 1703 (1990).
[9] P. Böni, J.H. Bilgram, and W. Känzig, Phys. Rev. A *28*, 2953 (1983); U. Dürig, J.H. Bilgram, W. Känzig, Phys. Rev. A *30*, 946 (1984); R. Steininger, J.H. Bilgram, J. Crystal Growth *112*, 203 (1991).
[10] J.-M. Laherrère, H. Savary, R. Mellet, and J.-C. Tolédano, Phys. Rev. A *41*, 1142 (1990).
[11] S. Hachisu, in: B.J. Ackerson (ed.) Phase Transitions *24*, No. 2–4, 1990.

Presented at the Discussion Meeting of the Deutsche Bunsen-Gesellschaft für Physikalische Chemie "Phase Transitions at Interfaces" in Bad Herrenalb, September 22nd to 24th, 1993 E 8560

Irreversible Multilayer Adsorption

P. Nielaba
Institut für Physik, KoMa 331, Universität Mainz, D-55099 Mainz, Germany

V. Privman
Physics Department, Clarkson University, Potsdam, NY 13699-5820, USA

J.-S. Wang
Computational Science, National University of Singapore, Kent Ridge, Singapore 0511

Key Words: Adsorption / Nonequilibrium Phenomena / Statistical Mechanics / Surfaces

Random sequential adsorption (RSA) models have been studied [1] due to their relevance to deposition processes on surfaces. The depositing particles are represented by hard-core extended objects; they are not allowed to overlap. Numerical Monte Carlo studies and analytical considerations are reported for 1D and 2D models of multilayer adsorption processes. Deposition without screening is investigated; in certain models the density may actually increase away from the substrate. Analytical studies of the late stage coverage behavior show the crossover from exponential time dependence for the lattice case to the power law behavior in the continuum deposition. 2D lattice and continuum simulations rule out some "exact" conjectures for the jamming coverage. For the deposition of dimers on a 1D lattice with diffusional relaxation we find that the limiting coverage (100%) is approached according to the $\sim 1/\sqrt{t}$ power-law preceded, for fast diffusion, by the mean-field crossover regime with the intermediate $\sim 1/t$ behavior. In case of k-mer deposition ($k > 3$) with diffusion the void fraction decreases according to the power-law $t^{-1/(k-1)}$. In the case of RSA of lattice hard squares in 2D with diffusional relaxation the approach to the full coverage is $\sim t^{-1/2}$. In case of RSA-deposition with diffusion of two by two square objects on a 2D square lattice the coverage also approaches 1 according to the power law $t^{-1/2}$, while on a finite periodic lattice the final state is a frozen random regular grid of domain walls connecting single site defects.

Ber. Bunsenges. Phys. Chem. 98, 451–454 (1994) No. 3 *0005-9021/94/0303-0451 $ 10.00+.25/0*